PANIC-4K: Upgrade with a HAWAII-4RG Array

Vianak Naranjo*[a], Armin Huber[a], Ulrich Mall[a], Richard J. Mathar[a], Peter Bizenberger[a]
[a]Max Planck Institute for Astronomy, Königstuhl 17, 69117 Heidelberg, Germany

ABSTRACT

PANIC[1], the PAnoramic Near-Infrared Camera for the Calar Alto Observatory in Spain, was successfully commissioned in late 2014 with a mosaic of four 2K x 2K HAWAII-2RG arrays covering a field of view of approximately 30 arcmin at the 2.2 m telescope. Unfortunately, two of its science detectors suffered from extreme degradation[2] along the years of operation making the instrument unsuitable for science observations. In the light of new technologies and constant innovations, it was decided to upgrade the instrument with a monolithic state of the art 4K x 4K HAWAII-4RG array. With as minimum mechanical and optical impact as possible for the instrument, the MPIA is the responsible institute for the challenging upgrade. Besides presenting the results of the initial operation of the HAWAII-4RG array in 64-Channel mode, the newly in-house designed detector mount will also be highlighted. In order to take as much advantage as possible of the new detector readout capabilities, and thanks to the modularity and flexibility of the in-house readout electronics, all 64 channels of the detector are read out in parallel. This allows for shorter integration times, which is very advantageous for a wide field imager with high background conditions.

Keywords: HAWAII-4RG, 64-channel mode, detector mount, integration time

1. INTRODUCTION

The complete PANIC instrument was shipped from the Calar Alto Observatory back to the MPIA in 2018 to upgrade the instrument by exchanging its mosaic of four H2RG arrays with a single HAWAII-4RG array. After re-integration at MPIA in September 2018, a dedicated test phase with the H4RG Multiplexer started in January 2019 and ended successfully in October that year with a fully functional H4RG Multiplexer at 80K in 64-channel mode parallel readout. At that moment the H4RG science grade array had just been delivered and its testing began early in 2020. Since the pixel pitch is of the new HAWAII-4RG array is slightly smaller than the original H2RG arrays (15 micron vs. 18 micron respectively), PANIC will lose a few arcminutes in its pixel scale, covering now a field of view of approximately 25 arcmin at the 2.2 m telescope and 12 arcmin at the 3.5 m telescope. This was the compromise that had to be made in order to avoid changes in the optical design[3]. Nevertheless, PANIC will still be one of the most powerful near infrared instruments of its class[3] in the operating wavelength range of 0.8 um to 2.5 um.

2. DETECTOR MOUNT

Upgrading the instrument with a new detector implies, at first glance and among others, many changes in the mechanical interfaces. In order to keep these changes to the minimum possible, it was clear that the first interface, the detector mount, had to be compatible with the original one.

The original detector mount housed four H2RG detectors and was built by GL Scientific, but the company was not available at the time of procuring the H4RG array. Therefore, MPIA decided to design its own mount.

The complete mount consists of two sub-assemblies: the detector module and the interface to the instrument.

*naranjo@mpia.de; phone +49 6221 528290; www.mpia.de

X-Ray, Optical, and Infrared Detectors for Astronomy IX, edited by Andrew D. Holland,
James Beletic, Proc. of SPIE Vol. 11454, 114542J · © 2020 SPIE
CCC code: 0277-786X/20/$21 · doi: 10.1117/12.2561424

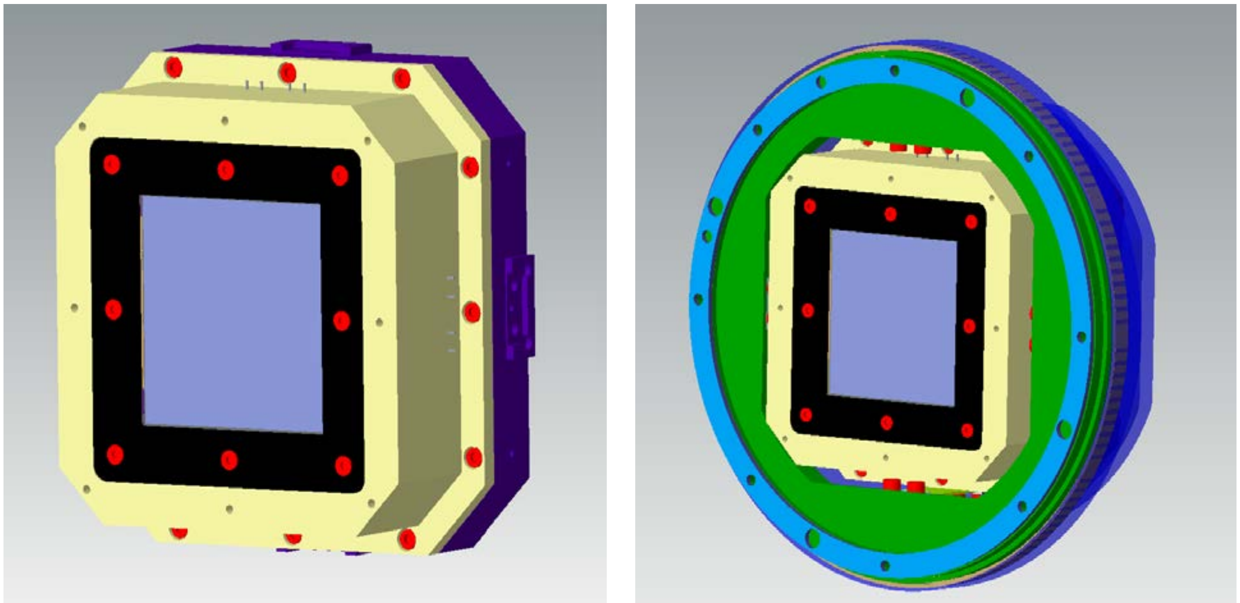

Figure 1. Detector module (left) assembled into the mounting interface to the instrument (right).

2.1 Detector module

The detector module houses the H4RG detector and includes heaters and temperature sensors for a two-stage temperature control loop. It consists of an aluminum base plate, an Invar plate, and a cover (see Figure 2). The Invar plate is attached by means of CuBe2 springs to the aluminum base plate. This plate is the support to which the detector is mounted; hence, the material was chosen to be the identical to the detector package in order to avoid stress due to different shrinkage rates during cool-down. Besides, the CuBe2 springs act as flexible elements to compensate for thermal shrinkage between the two plates. The main design driver was to avoid the introduction of stress and bending into the Invar plate and to define the thermal conductivity and the resulting cool down rate.

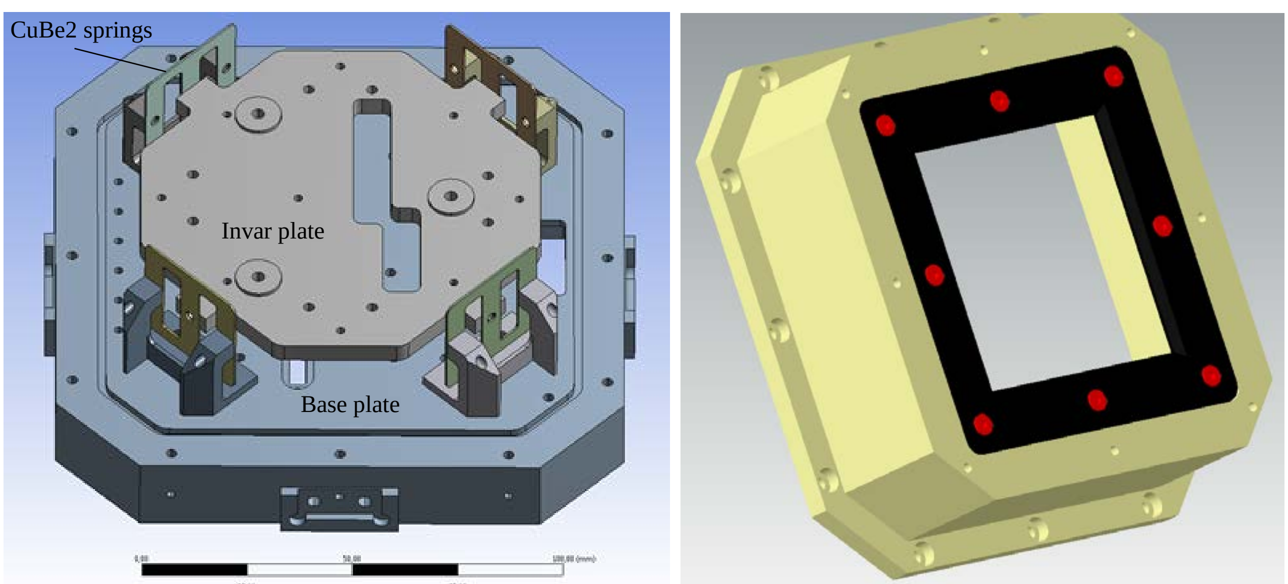

Figure 2. Aluminum base plate and Invar plate mounted on CuBe2 spring blades (left). Cover with field mask (right).

2.2 Mounting interface

The mounting interface is the mechanical interface between the detector module and the instrument structure. The detector module is mounted via four G10 struts to the mounting interface. These G10 struts insulate the detector module thermally and electrically from the instrument, allowing the detector to be operated at a different temperature than the instrument environment.

2.3 Thermal and deformation analysis

The following figures show the results obtained for the thermal distribution and deformation analysis of the detector module. The detector was considered as a point mass of 500 g, and the simulation was done considering a cool down temperature range from 22°C (295.15 K) to -193.15°C (80 K).

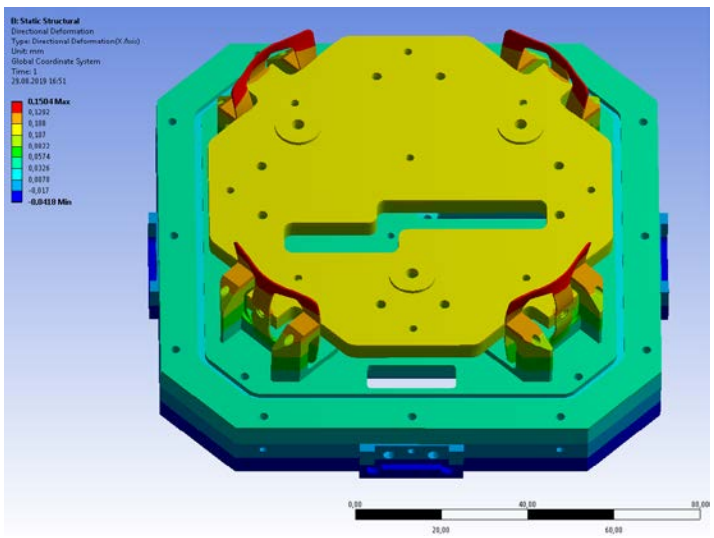

Figure 3. Deformation due to the cool down process along the optical axis. Under the given conditions the deformation of the Invar plate is very uniform.

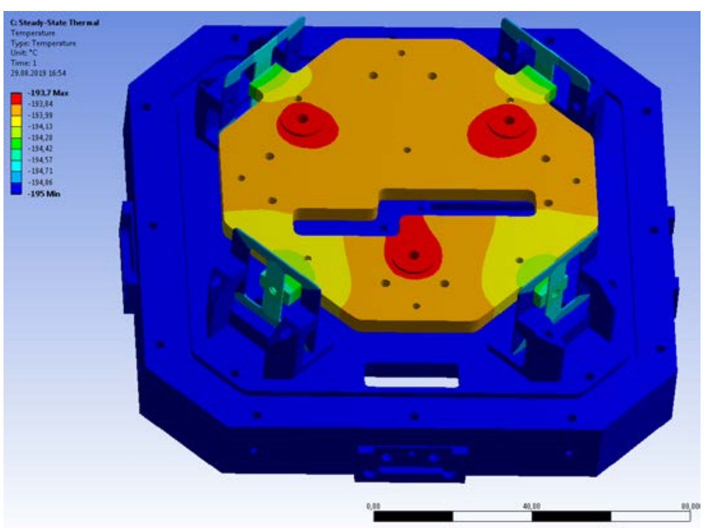

Figure 4. The temperature distribution shows a total gradient of ~1.3 K between the interface pads (red) of the Invar plate and the base plate (blue).

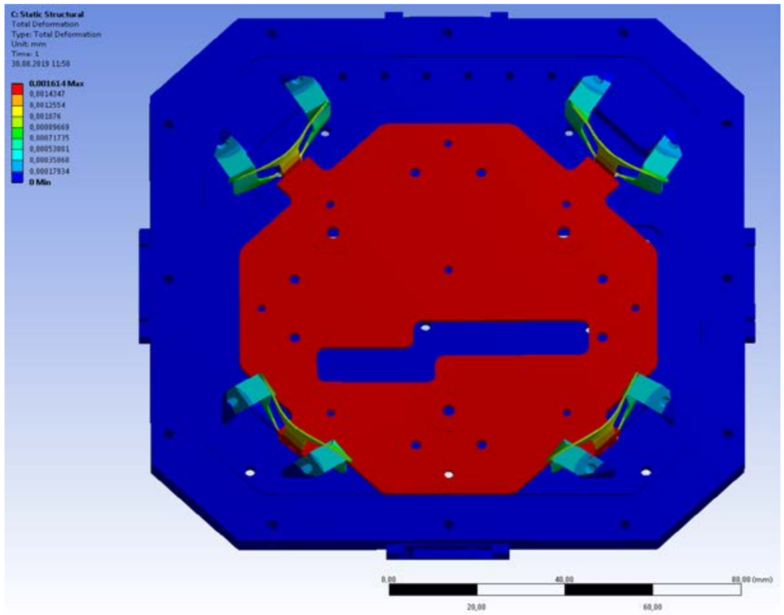

Figure 5. Deformation due to gravity at worst case: detector mount perpendicular to the ground. Due to self-weight deflection, the maximum bending is 1.6 µm.

A self-weight deflection analysis of the complete assembly (detector module and mounting interface) is presented in Figure 6. It shows that the maximum deflection is 22 µm. There is no tilt due to deflection introduced to the detector relative to the interface mount. It is a pure shift of the detector module.

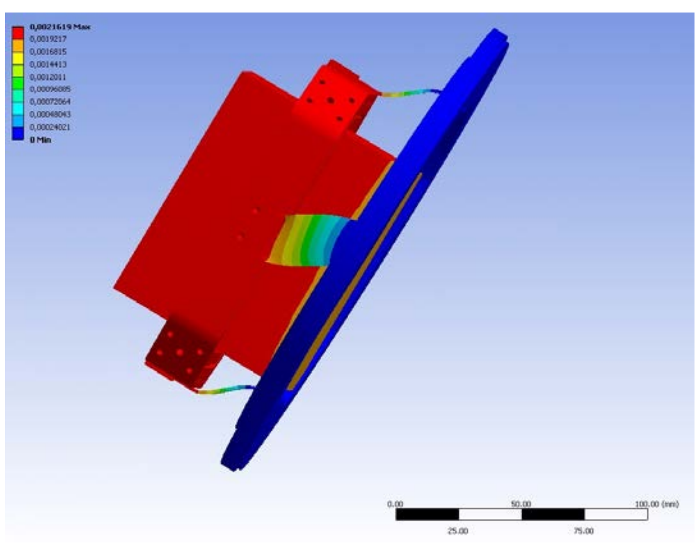

Figure 6. Result of the self-weight deflection analysis of the complete detector mount.

3. PRELIMINARY LAB RESULTS

The first test results were obtained during a test run in February early this year. Unfortunately, due to a series of unforeseen events during the first halve of this year and its inevitable consequences, it has been impossible to continue with the optimization and characterization of the PANIC H4RG array. Nevertheless, the preliminary results look very promising and the complete characterization of the array is planned for the first trimester of 2021.

3.1 Test setup

The tests were done using the final PANIC instrument and cryostat[5]. The readout mode used for the tests is the lir mode[6] operated at 100 kHz, reading in parallel all 64 channels "left to right" along the fast direction. An optimization of the bias voltages was not done at this point. The detector operating temperature was stabilized at 80 K.

3.2 Minimum integration times

Even though most of the measurements were done with the lir readout mode, basic function tests were also carried out with other standard MPIA readout modes[6]. The following table shows the minimum integration times for the readout modes used for the tests presented below.

Table 1. PANIC-4K minimum integration times

Readout mode	Minimum integration time (s)
lir	5.485574
rrr-mpia	2.743124

3.3 Reset level drift

The reset level corresponds to the offset level of the detector signal after a reset is applied to all its pixels. In double correlated read, the reset frame corresponds to the first frame that is read before signal integration occurs, and it is independent of the commanded integration time. Since the photon collecting time in a reset frame is always identical to the time that is needed to apply the reset to all the detector pixels[6], the mean signal of the reset frame should always be the same for every image taken within an exposure sequence of different integration times.

However, it was observed that the reset level drifts with increasing illumination, and that the behaviour is different from readout mode to readout mode (see Figure 7).

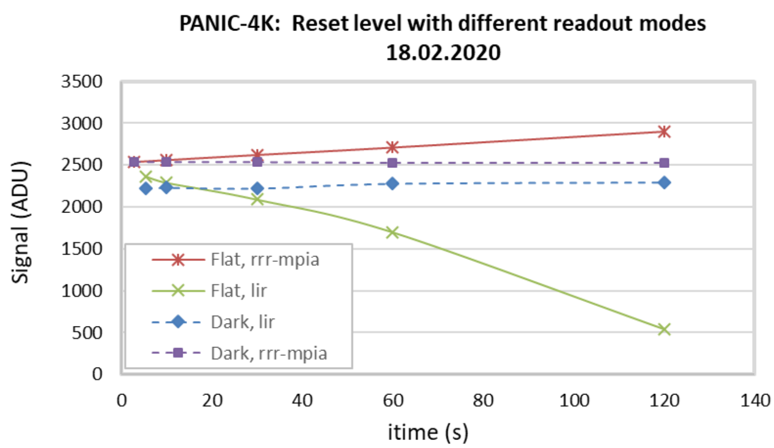

Figure 7. Reset level for flat field and dark, lir and rrr-mpia readout modes

Note that the reset level starts at about the same offset value for both readout modes (2500 ADU and 2200 ADU for the rrr-mpia and lir readout modes respectively) independently of the illumination conditions, but drifts away with increasing integration time for the flat exposures. The reset level increases with the integration time for the rrr-mpia readout mode, while it decreases dramatically for the lir readout mode. This behaviour will be further investigated during the next test phase in early 2021.

3.4 System gain

The system gain was calculated using the Photon Transfer Curve (variance vs. signal), keeping the illumination constant and varying only the detector integration time. The calculation was done for the whole array on a pixel-by-pixel basis, IPC correction was not done at this time. The estimated gain corresponds to 2.53 e-/ADU, as shown in Figure 8.

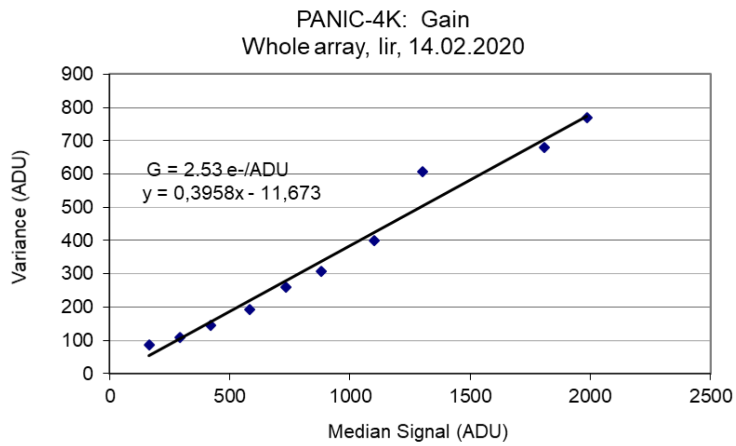

Figure 8. Photon transfer curve for gain estimation, lir readout mode

3.5 Full well capacity

A first rough estimation of the full well capacity was done by plotting the median output signal of the whole array vs. the detector integration time. The illumination was kept constant, varying only the detector integration time until fully saturating the array. As it can be observed in Figure 9, saturation occurs at ~ 43000 counts, which means that the full dynamic range of the 16 bit ADC[7] is not yet reached. This evidences the fact that the optimization of the system is still pending for the next test phase in early 2021.

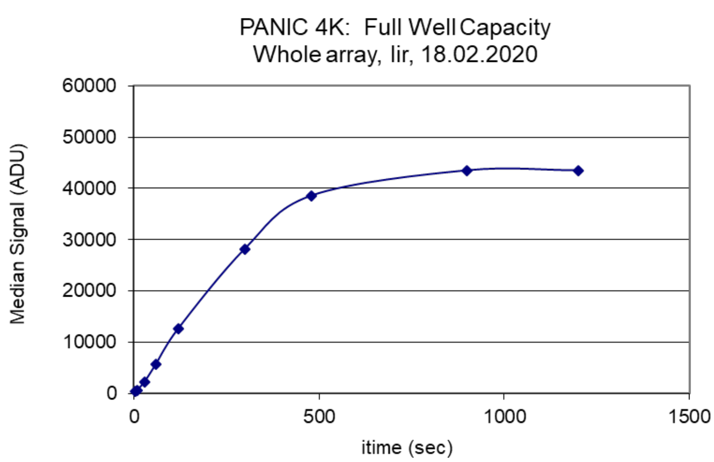

Figure 9. Plot of the signal vs. integration time for the estimation of the full well capacity, lir read out mode

3.6 Readout noise

The readout noise was calculated over a series of 20 dark frames obtained with minimum detector integration time and without any time interval between the individual frames, generating a noise frame in ADU on a pixel-by-pixel basis. After multiplying it by the system gain, its respective histogram (Figure 10) was calculated, showing that the temporal noise for the whole array corresponds to 14.9 e-.

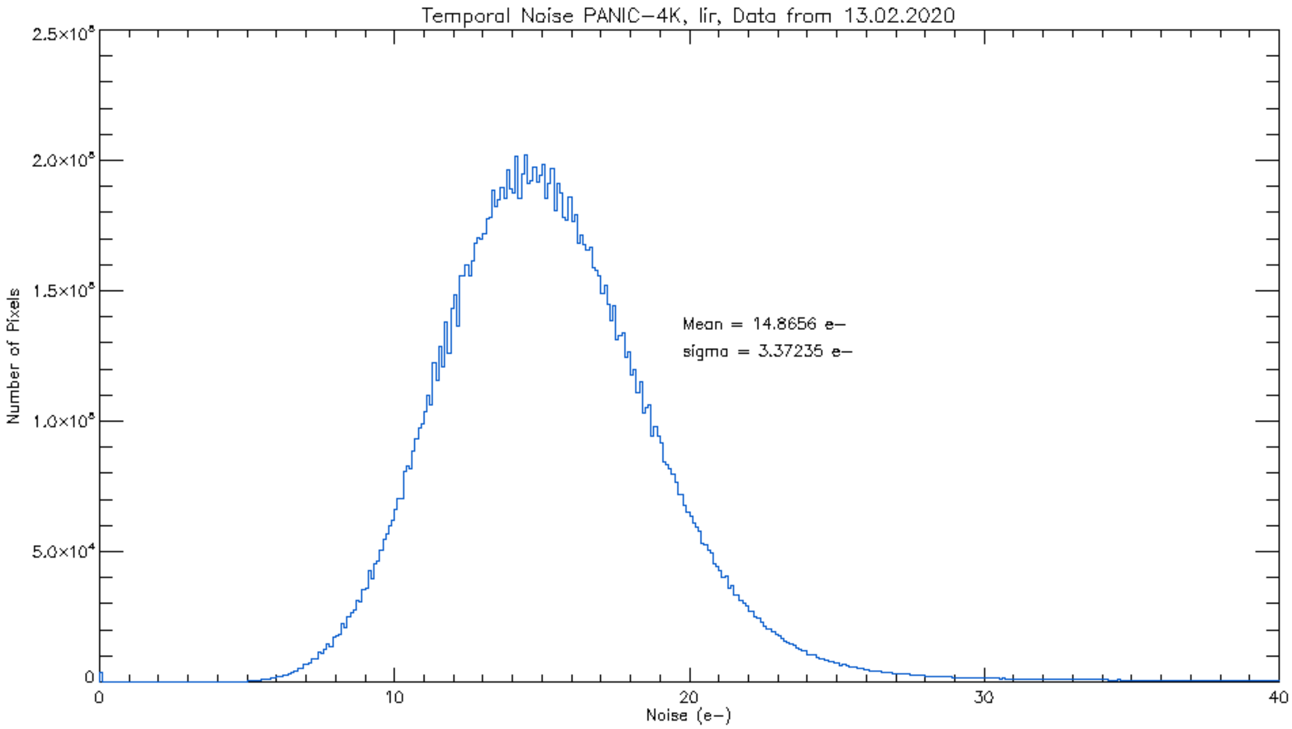

Figure 10. Histogram of the temporal noise over the whole array

4. CONCLUSIONS

The test results presented correspond to the first time that the PANIC-4K H4RG science detector was cooled down at MPIA. There was no optimization done, just a "plug and play" test phase to get a rough idea of the detector performance in combination with our readout system (electronics[7] and software[8]), and get a hint on where to start with troubleshooting, mitigation, and optimization. Based on the test results, there are two major issues that have to be addressed: the reset level drift has to be further investigated in order to evaluate possible mitigation strategies, and the full well capacity has to be optimized. There is still much work to be done, but the functionality of the HAWAII-4RG array in 64-channel mode with the MPIA in-house readout electronics and software was proven successful, and the basic performance of the detector was also satisfactory.

REFERENCES

[1] Baumeister, H., Alter, M., Cárdenas Vázquez, M. C., Fernández, M., Fried, J., Helmling, H., Huber, A., Ibáñez Mengual, J. M., Rodríguez Gómez, J. F., Laun, W., Lenzen, R., Mall, U., Naranjo, V., Ramos, J. R., Rohloff, R. R., Storz, C., Ubierna, M., Wagner, K., “PANIC: the new panoramic NIR camera for Calar Alto,” Proc. SPIE, Vol. 7014, 70142R (2008).

[2] Dorner, B., Huber, A, Cárdenas Vázquez, M. C., Ferro Rodriguez, I., Bizenberger, P., Naranjo, V., Panduro, J., Mall, U., Alter, M., Mathar, R. J., Storz, C., Rohloff, R. R., Fopp, P., Laun, W., Ibáñez, J. M., García Segura, A. J., Terrón, V., Fried, J. W., Fernández, M., Rodríguez Gómez, J. F., Meisenheimer, K., "PANIC in the lab: status before commissioning," Proc. SPIE 9147, 91473X (2014).

[3] Cárdenas Vázquez, M. C., Dorner, B., Huber, A., Sánchez-Blanco, E., Alter, M., Rodríguez Gómez, J. F., Bizenberger, P., Naranjo, V., Ibáñez Mengual, J. M., Panduro, J., García Segura, A. J., Mall, U., Fernández, M., Laun, W., Ferro Rodríguez, I. M., Helmling, J., Terrón, V., Meisenheimer, K., Fried, J. W., Mathar, R. J., Baumeister, H., Rohloff, R. R., Storz, C., Verdes-Montenegro, L., Bouy, H., Ubierna, M., Fopp, P., Funke, B., “PANIC: A General-purpose Panoramic Near-infrared Camera for the Calar Alto Observatory,” Publications of the Astronomical Society of the Pacific, Volume 130, Issue 984, pp. 025003 (2018).

[4] Cárdenas, M. C., Rodríguez Gómez, J., Lenzen, R., & Sánchez-Blanco, E., “Final Optical Design of PANIC, a Wide-Field Infrared Camera for CAHA,” 2010, ApSSP, 14, 471

[5] Fried, J. W., Baumeister, H., Huber, A., Laun, W., Rohloff, R. R., Cárdenas, M. C., “Opto-mechanical design of PANIC,” Proc. SPIE, Vol. 7735 (2010).

[6] Storz, C., Naranjo, V., Mall, U., Ramos, J., Bizenberger, P., Panduro, J., "Standard modes of MPIA's current H2/H2RG-readout systems," Proc. SPIE 8453, 84532E (2012).

[7] Wagner, K., Mall, U., Ramos J., Klein, R., “New Read-out electronics concept for visual and infrared detector arrays in astronomical instrumentation,” Proc. SPIE, Vol. 7014, 70145S (2008).

[8] Ibáñez Mengual, J. M., Fernández, M., Rodríguez Gómez, J. F., García, A. J., Storz, C., “The PANIC software system,” Proc. SPIE, Vol. 7740 (2010).